Understanding Temperature Stability of Surface Cation Dopants on LSCF Electrodes

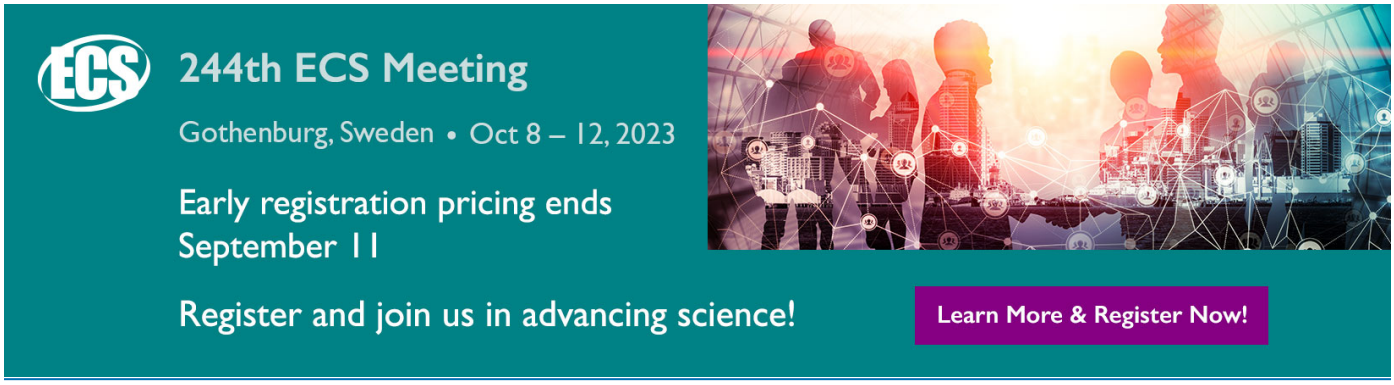

ECS Transactions, 111 (6) 2435-2443 (2023)
10.1149/11106.2435ecst ©The Electrochemical Society

Understanding Temperature Stability of Surface Cation Dopants on LSCF Electrodes

S. Coppieters 't Wallant[a], F. Grajkowski[b], B. Liu[a], O. Marina[c], L. Seymour[c], and B. Yildiz[a,d]

[a] Department of Materials Science and Engineering, Massachusetts Institute of Technology, Cambridge, Massachusetts 02139, USA
[b] Department of Chemistry, Massachusetts Institute of Technology, Cambridge, Massachusetts 02139, USA
[c] Pacific Northwest National Laboratory, Richland, Washington 99354, USA
[d] Department of Nuclear Science and Engineering, Massachusetts Institute of Technology, Cambridge, Massachusetts 02139, USA

State-of-the-art solid oxide fuel cell (SOFC) oxygen electrode materials such as $La_{0.6}Sr_{0.4}Co_{0.2}Fe_{0.8}O_{3-\delta}$ (LSCF) continue to be plagued by degradation primarily through strontium (Sr) segregation to the electrode surface and subsequent passivating poisoning reactions with chromium- and sulfur-containing species. Surface infiltration of more oxidizable cations is of interest for LSCF electrodes in order to reduce the electrostatic driver of Sr segregation and due its reported success in reducing Sr segregation and electrochemical degradation on LSC electrodes. In this work, we investigate the thermal stability of Hf, Nd, and Pr infiltrated cations at porous LSCF electrode surfaces. These select cations are of interest as surface infiltrates due to their more oxidizable nature. We demonstrate that infiltrated Hf, Nd, and Pr cations are not thermally stable at the LSCF electrode surface at standard SOFC operating temperatures, diffusing substantially away from the surface above 800°C.

Introduction

Fuel and electrolysis cells are a key technology for generating electricity as well as converting electricity to useful chemicals, including fuels such as hydrogen and syngas and chemicals such as ammonia and ethylene.[1,2] Solid oxide fuel and electrolysis technologies are of interest because of their high efficiencies compared to alkaline or PEM electrolysis, thanks to favorable thermodynamics and reaction kinetics at higher temperatures (650-800°C).[1]

The widespread application of solid oxide fuel cells (SOFCs) is largely inhibited by degradation issues with regards to the stability and oxygen exchange kinetics of the oxygen electrode. State-of-the-art SOFC materials such as $La_{0.6}Sr_{0.4}Co_{0.2}Fe_{0.8}O_{3-\delta}$ (LSCF) boast fast oxygen ion and electron conduction as well as high oxygen reduction activity.[1,3] But degradation issues continue to impede LSCF, primarily through strontium segregation to the electrode surface[4-8] and subsequent passivating poisoning reactions due to chromium- and sulfur-containing species.[9-11]

Previous work has demonstrated that the primary driving force of Sr segregation to perovskite oxide surfaces under cathodic polarization is the electrostatic interaction between the negatively-charged Sr lattice dopant cations with the positively-charged oxygen vacancies at the electrode surface.[12] In order to minimize this electrostatic segregation driver, the excess positive charge at the surface must be reduced. This work is motivated by exploring the possibility of utilizing a surface infiltration technique to suppress the electrostatic attraction of Sr to the surface and thus mitigate the detrimental Sr segregation at the oxygen electrode surface. Surface infiltration of more oxidizable cations would reduce the net excess positive charge at the electrode surface, thus reducing the electrostatic Sr segregation driver.

Deposition of more oxidizable cations (Zr, Hf, Ti, Nb) on $La_{0.8}Sr_{0.2}CoO_3$ (LSC) electrodes has been previously shown to improve the oxygen exchange kinetics and stability of the LSC electrode considerably.[13,14] Furthermore, significantly lower amounts of segregated SrO particles were found on LSC surfaces infiltrated with more oxidizable cations after testing.[13,14] The same reductions in Sr segregation have also been shown using Hf cations on LSM.[15]

In this work, we begin to investigate a solution infiltration technique to introduce cation dopants to the surface of LSCF porous electrodes on symmetrical cells to improve the stability and performance through suppression of Sr segregation. We explore both transition metal and lanthanide cations as more oxidizable infiltrated dopants on the porous LSCF electrode. Transition metal cations are of interest due to their more oxidizable nature and ability to reduce Sr segregation in LSC and LSM electrodes. More oxidizable lanthanide cations are of interest as more oxidizable cations of a considerably larger size than transition metal actions.

We present thermal stability studies of infiltrated transition metal and lanthanide cations infiltrated at the surface of the LSCF electrode. We demonstrate through X-ray photoelectron spectroscopy (XPS) analysis that Hf, Pr, and Nd cations are not thermally stable at the surface of LSCF electrodes above 800°C as said cations diffuse away from the electrode surface with increasing temperature. Furthermore, Sr segregates to the LSCF electrode surface more strongly with increasing temperature as the more oxidizable infiltrated cations diffuse away from the surface. Contrary to expectations from previous studies, these preliminary experiments demonstrate that select transition metal and lanthanide cation dopants diffuse into the LSCF lattice at standard SOFC operating temperatures. These thermal stability results will inform analysis of future electrochemical testing of LSCF symmetric cells infiltrated with more oxidizable transition metal or lanthanide cations.

Results

In this work, we investigate the surface of the $(La_{0.6}Sr_{0.4})_{0.95}Co_{0.2}Fe_{0.8}O_3$ (LSCF) and $Gd_{0.2}Ce_{0.8}O_{1.95}$ (GDC) composite oxygen electrode of a symmetric button cell (Figure 1a). LSCF/GDC electrodes are printed on scandium-stabilized zirconia (SSZ) electrolyte discs with a GDC barrier layer printed between the electrode and electrolyte layers (Figure 1a). SEM images of a symmetric button cell sample's cross section confirm proper contact

between the GDC barrier layer and SSZ electrolyte (Figure 1b). An aqueous solution infiltration method using transition metal- or lanthanide-chloride solutions is performed to infiltrate the LSCF/GDC electrode surface with transition metal or lanthanide cations. After infiltration, cells are annealed, resulting in a LSCF/GDC electrode infiltrated with transition metal or lanthanide cations.

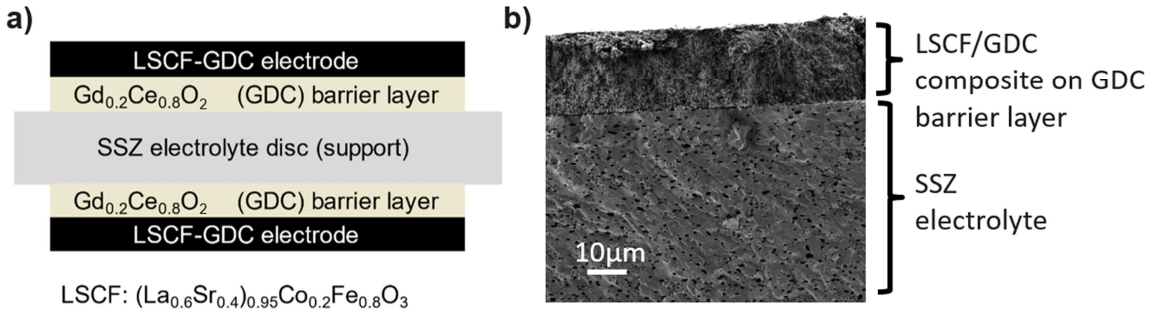

Figure 1. a) Schematic representation of symmetric button cell with scandium-stabilized zirconia (SSZ) electrolyte disc, $Gd_{0.2}Ce_{0.8}O_2$ (GDC) barrier layer, and $(La_{0.6}Sr_{0.4})_{0.95}Co_{0.2}Fe_{0.8}O_3$ (LSCF)/$Gd_{0.2}Ce_{0.8}O_2$ (GDC) composite electrodes. b) SEM image of symmetric cell cross section, with SSZ electrolyte and LSCF/GDC composite electrode with GDC barrier layer visible. Proper contact between the GDC barrier layer and SSZ electrolyte is visible.

In order to investigate the thermal stability of infiltrated surface cations on LSCF/GDC electrodes, we cyclically heat an infiltrated cell to a set temperature and, upon cooling to room temperature, perform XPS to probe the presence of the infiltrated cation and Sr at the surface post-heating. Upon each new heating cycle, the heating temperature is raised by 100°C. Cells are held at each set temperature for 3 hours.

We perform cyclic heating and XPS on a Hf-infiltrated LSCF/GDC composite electrode for a temperature range of 500°C to 800°C. The XPS analysis for Hf 4d region in Figure 2a demonstrates that the Hf 4d signal is reduced as temperature increases. This XPS result indicates diffusion of the surface infiltrated Hf cations into the LSCF/GDC electrode bulk with increasing temperature. Considerable Hf cation diffusion away from the surface is noticeable at 700°C and 800°C. Figure 2b shows the XPS analysis for Sr 3d region of the same Hf infiltrated sample. The feature associated with surface Sr species increases with increasing temperature. Thus, as Hf diffuses away from the electrode surface, Sr segregates more strongly to the surface.

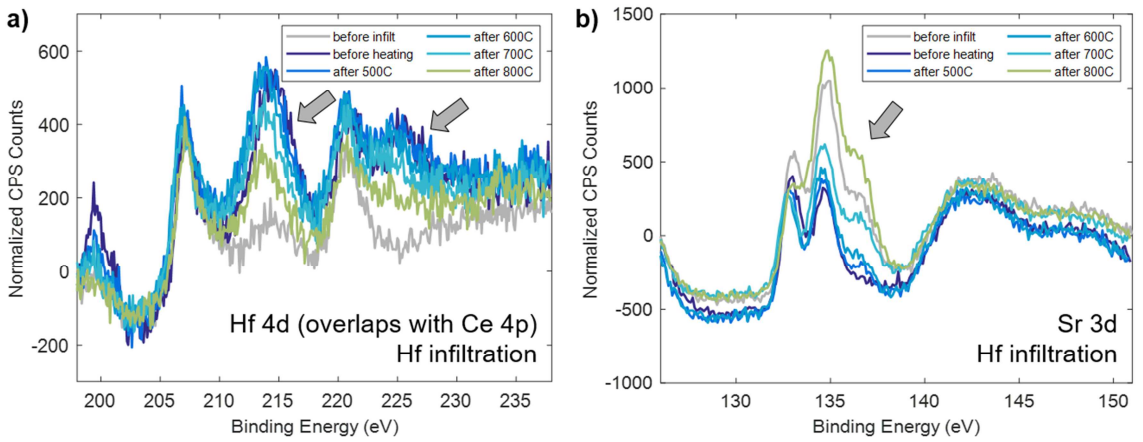

Figure 2. a) XPS analysis for Hf 4d region for a Hf-infiltrated sample (0.1M precursor solution, 2-minute soaking time), as a function of the highest temperature that the sample was exposed to. 'Before infilt.' refers to the sample in its as-prepared state before infiltration and 'before heating' refers to the sample after infiltration but before any heating. The Hf 4d peaks of interest are indicated by grey arrows. b) XPS analysis of the Sr 3d region for the same Hf-infiltrated sample. The Sr 3d feature associated with surface Sr species is indicated by a grey arrow.

Cyclic heating and XPS is performed on a Pr infiltrated LSCF/GDC composite electrode for a temperature range of 500°C to 1000°C. The XPS analysis for Pr 3d region in Figure 3a reveals a reduction in the Pr 3d signal with increasing temperature, with Pr 3d signal appearing nearly depleted at 900°C and 1000°C. These results indicate diffusion of the surface infiltrated Pr cations into the LSCF/GDC electrode bulk with increasing temperature. Much like with the Hf-infiltrated sample, the surface component of the Sr 3d signal of the Pr infiltrated sample increases with increasing temperature (Figure 3b). We demonstrate that as Pr cations diffuse away from the electrode surface, Sr segregates more strongly to the surface.

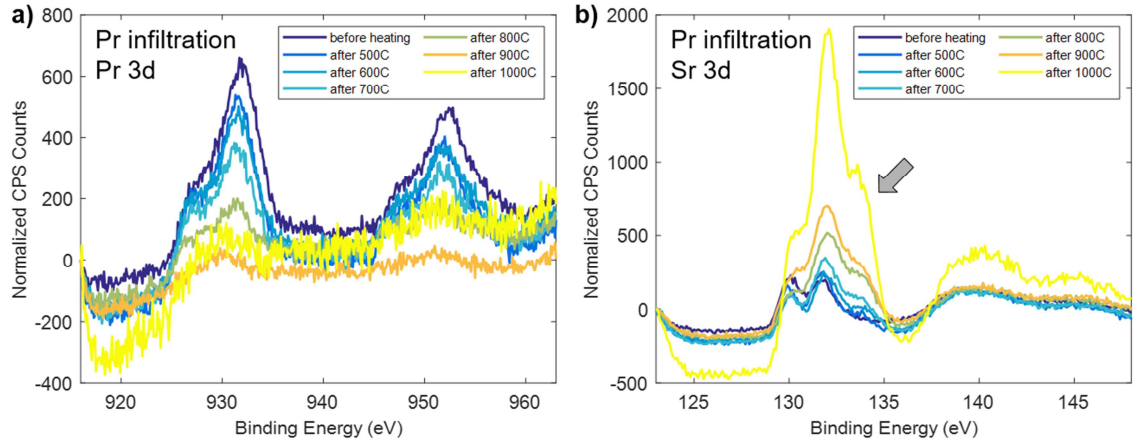

Figure 3. a) XPS analysis for Pr 3d region for a Pr-infiltrated sample (0.025M precursor solution, 5-minute soaking time), as a function of the highest temperature that the sample was exposed to. 'Before heating' refers to the sample after infiltration but before any heating. b) XPS analysis of the Sr 3d region for the same Pr-infiltrated sample. The Sr 3d feature associated with surface Sr species is indicated by a grey arrow.

The final infiltration chemistry we explore is Nd infiltration. The Nd-infiltrated LSCF/GDC electrode sample is tested from 500°C to 1000°C. The XPS analysis in Figure 4a shows that the Nd 3d signal is reduced as temperature increases, suggesting diffusion of Nd cations from the surface into the bulk of the LSCF/GDC electrode. By 900°C, Nd appears to have nearly completely diffused away from the surface as the Nd 3d signal becomes comparable to the pre-infiltration signal. Figure 2b shows the XPS analysis for Sr 3d region of the same Nd infiltrated sample. The feature associated with surface Sr species increases with increasing temperature, indicating that as Nd diffuses away from the electrode surface, Sr segregates more strongly to the surface.

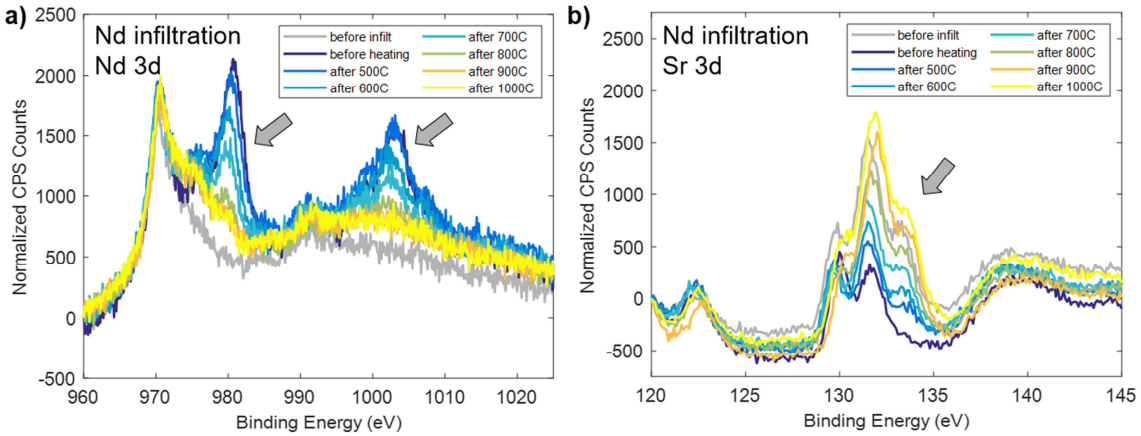

Figure 4. a) XPS analysis for Nd 3d region for a Nd-infiltrated sample (0.025M precursor solution, 5-minute soaking time), as a function of the highest temperature that the sample was exposed to. 'Before infilt.' refers to the sample in its as-prepared state before infiltration and 'before heating' refers to the sample after infiltration but before any heating. The Nd 3d peaks of interest are indicated by grey arrows. b) XPS analysis of the Sr 3d region for the same Nd-infiltrated sample. The Sr 3d feature associated with surface Sr species is indicated by a grey arrow.

Nd infiltration is performed on both a pure LSCF electrode and a LSCF/GDC composite electrode to begin to elucidate the role that GDC may play in the diffusion of surface infiltrated cations into the electrode bulk. In Figure 5a, Nd 3d XPS signal is presented for a Nd-infiltrated pure LSCF electrode at temperatures from 500°C to 1000°C. In Figure 5b, Nd 3d XPS signal is presented for a Nd-infiltrated LSCF/GDC composite electrode at temperatures from 500°C to 1000°C. In both the pure LSCF and LSCF/GDC electrode samples, the Nd 3d signal appears largely depleted above 800°C (Figure 5). We observe no substantial differences in the presence of Nd cations at the surface with increasing temperature between the pure LSCF and LSCF/GDC composite electrodes. These initial results suggest that surface Nd cation diffusion is not likely dominated by diffusion through GDC particles in the electrode.

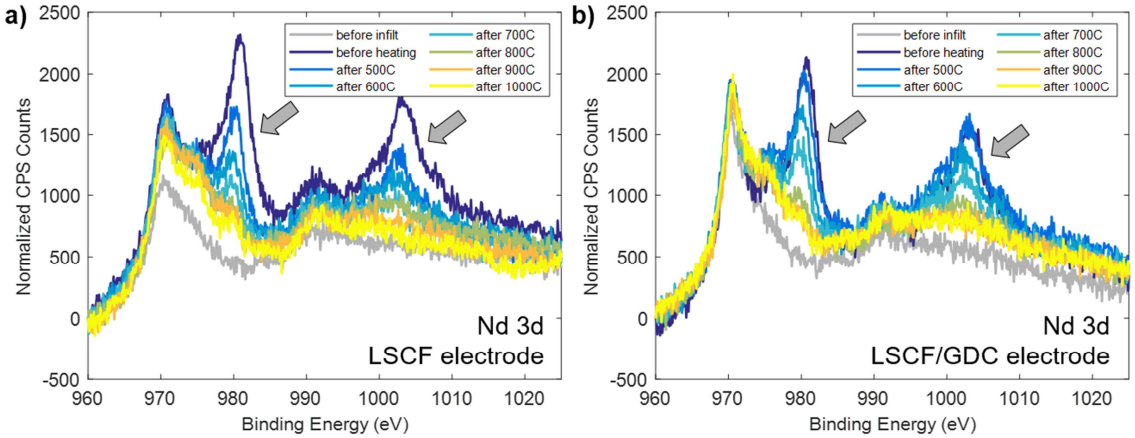

Figure 5. a) XPS analysis for Nd 3d region for a Nd-infiltrated sample (0.025M precursor solution, 5-minute soaking time) with a pure LSCF electrode, as a function of the highest temperature that the sample was exposed to. 'Before infilt.' refers to the sample in its as-prepared state before infiltration and 'before heating' refers to the sample after infiltration but before any heating. The Nd 3d peaks of interest are indicated by grey arrows. b) XPS analysis of the Nd 3d region for a Nd-infiltrated sample (0.025M precursor solution, 2-minute soaking time) with a LSCF/GDC composite electrode. The Nd 3d peaks of interest are indicated by grey arrows.

Discussion

We find that infiltrated surface Hf diffuses into the porous LSCF/GDC cathode bulk with increasing temperature while Sr segregates more and more strongly to the surface (Figure 1). Given that previous work has demonstrated substantial improvement of oxygen exchange kinetics and stability of LSC electrodes upon deposition of more oxidizable cations (Zr, Hf, Ti, Nb),[13,14] it is surprising to find that Hf cations are not thermally stable at comparable temperatures on the surface of LSCF/GDC electrodes.

Given these diffusion results for Hf, a transition metal dopant, we previously hypothesized that lanthanide cation dopants may be less likely to diffuse into the cathode bulk due to their larger cation size. However, Pr- and Nd- infiltrated LSCF/GDC electrodes demonstrate similar thermal stability trends for the infiltrated surface cations, with substantial diffusion of Nd and Pr into the electrode bulk above 800°C (Figures 3 and 4).

In order to begin exploring potential diffusion pathways for the infiltrated cations, we perform temperature studies of Nd-infiltrated pure LSCF and LSCF/GDC composite cathodes. We observe diffusion of Nd into the electrode bulk on both the LSCF and LSCF/GDC electrodes, with Nd appearing to have almost completely diffused at 800°C for both electrodes. These initial results suggest that diffusion is not likely dominated by diffusion through GDC particles in the electrode lattice.

The results of this study are relevant to inform upcoming electrochemical studies of symmetric LSCF electrode cells infiltrated with transition metal or lanthanide cations to suppress Sr segregation. If infiltrated cells demonstrate changes in electrochemical stability or performance at normal operating temperatures (800°C), the sub-surface

influence of these dopants must be considered. This is contrary to previous assumptions that the electrochemical impacts of these cation infiltrates at SOFC operating temperatures would likely be surface impacts. These preliminary cation thermal stability studies lay the groundwork for understanding future electrochemical testing of LSCF symmetric cells infiltrated with more oxidizable transition metal or lanthanide cations.

Materials and Methods

Sample Preparation

Cell Fabrication. SSZ electrolyte discs, $(La_{0.6}Sr_{0.4})_{0.95}Co_{0.2}Fe_{0.8}O_3$ (LSCF) powder, and ink vehicle are sourced from fuelcellmaterials. $Gd_{0.2}Ce_{0.8}O_2$ (GDC) powder was made via a combustion sol-gel procedure from an aqueous solution. Appropriate amounts of $Ce(NO_3)_3 \cdot 6H_2O$ and $Gd(NO_3)_3 \cdot 6H_2O$ were dissolved in DI water to which citric acid was added in a 1.1:1 metal salt:citric acid ratio. The solution was then heated, forming a gel which dried with heating and then underwent self-combustion. The resulting loose debris was collected into an alumina crucible and heated to 350°C for 4 hours and 1050°C for 5 hours and subsequently ball-milled.

Both the barrier layer and electrode are screen printed onto the SSZ electrolyte disc. For the GDC barrier layer, an ink consisting of an ink vehicle to GDC mass ratio of 1:1.5 is made and screen printed directly on the SSZ electrolyte disc. After drying, the sample is placed in an alumina crucible and heated to 1400°C for 5 hours to sinter the GDC barrier layer. The electrode layer is screen printed next. For the LSCF/GDC composite electrode, an ink consisting of a LSCF:GDC:ink vehicle mass ratio of 1:1:1 is made and screen printed on top of the sintered GDC barrier layer. For the pure LSCF electrode, an ink consisting of a LSCF:ink vehicle mass ratio of 2:1 is made and screen printed on top of the sintered GDC barrier layer. After drying of the electrode layer, the sample is placed in an alumina crucible and heated to 1100°C for 2 hours to sinter the electrode layer.

Infiltration. An aqueous precursor solution is made: 0.1M hafnium chloride, 0.025M praseodymium (III) chloride, and 0.025M neodymium (III) chloride, respectively. The button cell is submerged vertically in the precursor solution for 2 minutes for Hf infiltration and 5 minutes for Pr and Nd infiltrations. The sample is then dipped vertically into IPA for 5 seconds and subsequently dipped vertically into DI water for 5 seconds as rinsing steps. The sample is then annealed in an alumina crucible on a hot plate at 250°C for 15 minutes and then allowed to cool slowly to room temperature.

XPS Measurements and Analysis

Ex-situ x-ray photoelectron spectroscopy on the surface of pure LSCF and LSCF/GDC composite porous electrodes is performed using PHI Versaprobe II XPS with a mono-energetic Al Kα x-rays source. C60 cluster-ion gun is used to neutralize surface charges and allow photoelectron emission. Fitting and quantitative analysis of XPS spectra is performed with CasaXPS software. XPS measurements are performed at room temperature and base pressure of 10^{-10} Torr.

Conclusion

In this work, we investigate the thermal stability of infiltrated transition metal and lanthanide cations at the surface of the LSCF electrode. We utilize a solution infiltration technique to introduce cation dopants to the surface of LSCF porous electrodes, which is of interest due to previous work demonstrating improved oxygen exchange kinetics and stability of LSC electrodes infiltrated with more oxidizable transition metal cations at the surface through suppression of Sr segregation. We demonstrate through XPS analysis that Hf, Pr, and Nd cations are not thermally stable at the surface of LSCF electrodes above 800°C as said cations diffuse away from the electrode surface with increasing temperature. Furthermore, Sr segregates to the LSCF electrode surface more strongly with increasing temperature, as the more oxidizable infiltrated cations diffuse away from the surface. These thermal stability results will inform analysis of future electrochemical testing of LSCF symmetric cells infiltrated with more oxidizable transition metal or lanthanide cations.

Acknowledgments

This study is supported by the U.S. Department of Energy – NETL DE-FE0032102. The authors acknowledge the use of the Materials Research Laboratory, an MRSEC Shared Experimental Facility of the NSF at MIT, supported by the NSF under award number DMR-1419807.

References

1. A. Hauch, R. Kungas, P. Blennow, A. B. Hansen, J. B. Hansen, B. V. Mathiesen, and M. B. Mogensen, *Science*, **370** (2020).
2. J. B. Hansen, *Faraday Discuss.*, **182**, 9-48 (2015).
3. A. J. Jacobson, *Chemistry of Materials*, **22**, 660-674 (2009).
4. S. P. Simner, M. D. Anderson, M. H. Engelhard, and J. W. Stevenson, *Electrochemical and Solid State Letters*, **9** (2006).
5. Y. Liu, K. Chen, L. Zhao, B. Chi, J. Pu, S. P. Jiang, and L. Jian, *International Journal of Hydrogen Energy*, **39** (2014).
6. T. T. Fister, D. D. Fong, J. A. Eastman, P. M. Baldo, M. J. Highland, P. H. Fuoss, K. R. Balasubramaniam, J. C. Meador, and P. A. Salvador, *Appl. Phys. Lett.*, **93** (2008).
7. K. Katsiev, B. Yildiz, K. Balasubramaniam, and P. A. Salvador, *Appl. Phys. Lett.*, **95** (2009).
8. B. Yildiz, K.-C. Chang, D. Myers, J. D. Carter, and H. You, *Advances in Solid Oxide Fuel Cells III: Ceramic Engineering and Science Proceedings*, **28** (2007).
9. F. Wang, H. Kishimoto, K. Develos-Bagarinao, K. Yamaji, T. Horita, and H. Yokokawa, *Journal of The Electrochemical Society*, **163** (2016).
10. K. Chen and S. P. Jiang, *Electrochemical Energy Reviews*, **3**, 730-765 (2020).
11. S. P. Jiang and X. Chen, *International Journal of Hydrogen Energy*, **39**, 505-531 (2014).

12. D. Kim, R. Bliem, F. Hess, J.-J. Gallet, and B. Yildiz, *J. Am. Chem. Soc*., **142,** 3548-3563 (2020).
13. N. Tsvetkov, Q. Lu, L. Sun, E.J. Crumlin, and B. Yildiz, *Nat. Mater*., **15**, 1010-1016 (2016).
14. N. Tsvetkov, Q. Lu, and B. Yildiz, *Faraday Discussions*, **182**, 257-269 (2015).
15. R. Bliem, D. Kim, J. Wang, E. J. Crumlin, and B. Yildiz, *The Journal of Physical Chemistry C*, **125**, 3346-3354 (2021).